© American College of Medical Genetics and Genomics

ORIGINAL RESEARCH ARTICLE | Genetics inMedicine

Arterial tortuosity syndrome: 40 new families and literature review

Aude Beyens, MD[1], Juliette Albuisson, MD, PhD[2], Annekatrien Boel, MSc[1], Mazen Al-Essa, MD[3], Waheed Al-Manea, MD[4], Damien Bonnet, MD, PhD[5], Ozlem Bostan, MD[6], Odile Boute, MD[7], Tiffany Busa, MD[8], Nathalie Canham, MD[9], Ergun Cil, MD, PhD[6], Paul J. Coucke, PhD[1], Margot A. Cousin, MD[10,11], Majed Dasouki, MD[12], Julie De Backer, MD, PhD[1,13], Anne De Paepe, MD, PhD[1], Sofie De Schepper, MD, PhD[14], Deepthi De Silva, MBChB, MRCP[15,16], Koenraad Devriendt, MD, PhD[17], Inge De Wandele, PhD[1], David R. Deyle, MD[10,18,19], Harry Dietz, MD, PhD[20], Sophie Dupuis-Girod, MD[21], Eudice Fontenot, MD[22], Björn Fischer-Zirnsak, PhD[23], Alper Gezdirici, MD[24], Jamal Ghoumid, MD, PhD[25], Fabienne Giuliano, MD[26], Neus Baena Diéz, PhD, MD[27], Mohammed Z. Haider, MD, PhD[3], Joshua S. Hardin, MD[28], Xavier Jeunemaitre, MD, PhD[2], Eric W. Klee, PhD[10,11,18], Uwe Kornak, MD, PhD[23], Manuel F. Landecho, MD, PhD[29], Anne Legrand, MD[2], Bart Loeys, MD, PhD[30], Stanislas Lyonnet, MD, PhD[31], Helen Michael, MD[32], Pamela Moceri, MD[33], Shehla Mohammed, MD[34], Laura Muiño-Mosquera, MD[1], Sheela Nampoothiri, MD, PhD[35], Karin Pichler, MD, PhD[36], Katrina Prescott, MD[37], Anna Rajeb, MD, PhD[23], Maria Ramos-Arroyo, MD[38], Massimiliano Rossi, MD[39], Mustafa Salih, MD[40], Mohammed Z. Seidahmed, MD[4], Elise Schaefer, MD[41], Elisabeth Steichen-Gersdorf, MD[36], Sehime Temel, MD, PhD[42,43,44], Fahrettin Uysal, MD[6], Marine Vanhomwegen, BSc[1], Lut Van Laer, PhD[30], Lionel Van Maldergem, MD, PhD[45], David Warner, MD[28], Andy Willaert, PhD[1], Tom R. Collins, II, MD[22], Andrea Taylor, BN[46], Elaine C. Davis, PhD[47], Yuri Zarate, MD[10] and Bert Callewaert, MD, PhD[1]

Purpose: We delineate the clinical spectrum and describe the histology in arterial tortuosity syndrome (ATS), a rare connective tissue disorder characterized by tortuosity of the large and medium-sized arteries, caused by mutations in *SLC2A10*.

Methods: We retrospectively characterized 40 novel ATS families (50 patients) and reviewed the 52 previously reported patients. We performed histology and electron microscopy (EM) on skin and vascular biopsies and evaluated TGF-β signaling with immunohistochemistry for pSMAD2 and CTGF.

Results: Stenoses, tortuosity, and aneurysm formation are widespread occurrences. Severe but rare vascular complications include early and aggressive aortic root aneurysms, neonatal intracranial bleeding, ischemic stroke, and gastric perforation. Thus far, no reports unequivocally document vascular dissections or ruptures. Of note, diaphragmatic hernia and infant respiratory distress syndrome (IRDS) are frequently observed. Skin and vascular biopsies show fragmented elastic fibers (EF) and increased collagen deposition. EM of skin EF shows a fragmented elastin core and a peripheral mantle of microfibrils of random directionality. Skin and end-stage diseased vascular tissue do not indicate increased TGF-β signaling.

Conclusion: Our findings warrant attention for IRDS and diaphragmatic hernia, close monitoring of the aortic root early in life, and extensive vascular imaging afterwards. EM on skin biopsies shows disease-specific abnormalities.

Genet Med advance online publication 11 January 2018

Key Words: aneurysm; arterial tortuosity syndrome; electron microscopy; GLUT10; *SLC2A10*

[1]Center For Medical Genetics Ghent, Ghent University Hospital, Ghent, Belgium; [2]APH, Hôpital Européen Georges Pompidou, Centre de Référence des Maladies Vasculaires Rares, INSERM, U970, Université Descartes Paris, Sarbonne Cité, Paris, France; [3]Pediatrics Department, Kuwait University, Kuwait City, Kuwait; [4]Pediatric Department, Security Forces Hospital, Riyadh, Kingdom of Saudi Arabia; [5]Medical Genetics Service, Hôpital Necker-Enfants Malades, Paris, France; [6]Department of Pediatric Cardiology, University of Uludag, Bursa, Turkey; [7]Clinical Genetics Service "Guy Fontaine," Hôpital Calmette, Lille, France; [8]Service de Génétique Clinique, Département de Génétique, AP-HM CHU Timone Enfants, Marseille, France; [9]North West Thames Regional Genetics Service, Northwick Park Hospital, Harrow, United Kingdom; [10]Department of Health Sciences Research, Mayo Clinic, Rochester, Minnesota, USA; [11]Center for Individualized Medicine, Mayo Clinic, Rochester, Minnesota, USA; [12]Department of Pediatrics, University of Kansas, Kansas City, Kansas, USA; [13]Department of Cardiology, Ghent University Hospital, Ghent, Belgium; [14]Department of Dermatology, Ghent University Hospital, Ghent, Belgium; [15]Department of Physiology, University of Kelaniya, Ragama, Sri Lanka; [16]Faculty of Medicine, University of Kelaniya, Ragama, Sri Lanka; [17]Center for Human Genetics, Leuven University Hospital, Leuven, Belgium; [18]Department of Clinical Genomics, Mayo Clinic, Rochester, Minnesota, USA; [19]Department of Molecular Medicine, Mayo Clinic, Rochester, Minnesota, USA; [20]Department of Pediatrics, Johns Hopkins University School of Medicine, Baltimore, Maryland, USA; [21]Hospices Civils de Lyon, Hôpital Femme-Mère-Enfants, Service de Génétique et Centre de Référence Pour la Maladie de Rendu-Osler, Université Lyon, Lyon, France; [22]Division of Cardiology, Department of Pediatrics, University of Arkansas for Medical Sciences, Little Rock, Arkansas, USA; [23]Institute of Medical and Human Genetics, Charité-Universitätsmedizin Berlin, Berlin, Germany; [24]Department of Medical Genetics, Kanuni Sultan Suleyman Training and Research Hospital, Istanbul, Turkey; [25]Department of Medical Genetics, Lille University Hospital, CHU Lille, Lille, France; [26]Department of Physical Medicine and Rehabilitation, Raymond Poincare Hospital, Garches, France; [27]Genetics Laboratory UDIAT Diagnostic Center, Parc Tauli University Hospital, Sabadell, Spain; [28]Department of Ophthalmology, Arkansas Children's Hospital, Little Rock, Arkansas, USA; [29]Department of Internal Medicine, Clínica Universidad de Navarra, Pamplona,

INTRODUCTION

Arterial tortuosity syndrome (ATS, MIM 208050) is a rare, autosomal recessive connective tissue disorder characterized by elongated and tortuous large and medium-sized arteries with a propensity for aneurysm formation, dissection, and ischemic events.[1–7] Arterial narrowing, both locally and over longer stretches, may be associated, mainly in the pulmonary arteries and the aorta. Patients usually present with suggestive craniofacial and connective tissue manifestations such as a hyperextensible skin, cutis laxa, diaphragmatic hernia, and Marfanoid skeletal features.[1,4–14] Initial reports describe a poor prognosis with mortality rates up to 40% before the age of 5 years,[7] but subsequent series suggest a milder course.[15] Despite the description of 38 probands to date, the clinical spectrum and natural history are incompletely studied and therefore, clinical management relies mainly on expert opinion.

ATS is caused by loss-of-function mutations in the *SLC2A10* gene (MIM 606145) encoding the facilitative glucose transporter GLUT10.[16] The substrate and intracellular location(s) of GLUT10 remain uncertain, and as a consequence, the pathogenesis elusive. The main hypothesis depicts GLUT10 as a transporter of dehydroxyascorbic acid that may be present both over the mitochondrial membranes and the endoplasmic reticulum. In mitochondria, reduced dehydroxyascorbic acid or ascorbic acid acts as a reactive oxygen species scavenger, which protects cells against oxidative stress. In the endoplasmic reticulum, ascorbic acid functions as a hydroxylation cofactor for both prolyl and lysyl residues, which in its turn is a crucial reaction for elastin and collagen maturation.[17] Histopathology of affected vessel walls reveals fragmentation of the internal elastic lamina and elastic laminae of the tunica media of the large arteries,[2,4–6,8,9,12,14] but the consequences at the ultrastructural level have not been described. Several connective tissue disorders associated with arterial tortuosity and aneurysm formation show considerable clinical, histological, and pathophysiological overlap with ATS. These include autosomal recessive cutis laxa type 1b (MIM 219100) caused by *FBLN4* mutations (MIM 604633) and Loeys–Dietz syndrome (MIM 609192).[18,19] Furthermore, these disorders show upregulation of the TGF-β signaling pathway in vascular tissue affected by end-stage disease. However, a morpholino knockdown zebrafish model for ATS suggested reduced TGF-β signaling during initial developmental stages.[20] This study reports the clinical and molecular data for 40 newly identified ATS families including 50 affected individuals. In addition, we performed a clinical review of 52 patients described in the literature.

MATERIALS AND METHODS

Patients

All the included patients harbor biallelic *SLC2A10* mutations. Informed consent was obtained from all subjects or from their parents for minor patients, including specific consent to publish clinical pictures in **Figure 1**. Clinical information and cardiovascular imaging data were retrospectively obtained from trained clinicians at the referral centers using a checklist (**Supplementary Table S1** online). When available, clinical photographs and cardiovascular imaging data were reviewed by B.C. to minimize interobserver variability. In addition, we reviewed the data for all 52 previously reported patients with confirmed *SLC2A10* mutations, using the same methodology. Proband F21 was published previously as a short case report,[21] but we provide more extensive clinical data here. This study was approved by the Ghent University Hospital and Arkansas Children's Hospital ethical committees (registration number B670201319336).

Molecular analysis

Genomic DNA was extracted from blood samples using standard procedures. The *SLC2A10* gene was amplified by polymerase chain reaction (primers available on request) and polymerase chain reaction products were sequenced using next-generation sequencing (MiSeq, Illumina, San Diego, CA, USA) and compared with the wild-type sequence as submitted by the Genbank accession number NM_030777.3.[15] Complementary DNA numbering starts at the first nucleotide of the ATG start codon and protein annotation starts at the first methionine.

Histology and electron microscopy

We obtained skin biopsies of probands F30, F33, and F34, pulmonary artery biopsies of patient F12:V-2, F21, and F34, and an aortic biopsy of patient F22. A skin control sample was obtained from an age- and sex-matched patient referred for exclusion of systemic lupus erythematosus, control pulmonary arteries biopsies were obtained from an age-matched patient with ornithine transcarbamylase deficiency, and control aorta was obtained from an age-matched patient with suspected vascular Ehlers–Danlos syndrome with normal elastic fibers on orcein staining (two different

Spain; [30]Center of Medical Genetics, University Hospital of Antwerp, Antwerp, Belgium; [31]Medical Genetics Service, Hôpital Necker–Enfants Malades, Paris, France; [32]Paediatric Cardiology and Transition, Leeds General Infirmary, Leeds, United Kingdom; [33]Cardiology Department, Université Côte d'Azur, CHU de Nice et Hôpitaux Universitaires Pédiatriques Lenval, Nice, France; [34]South East Thames Regional Genetics Service, Guy's Hospital, London, United Kingdom; [35]Department of Pediatric Genetics, Amrita Institute of Medical Sciences and Research Center, Cochin, Kerala, India; [36]Clinic for Pediatrics I, Medical University of Innsbruck, Innsbruck, Austria; [37]Clinical Genetics, Yorkshire Regional Genetics Service, Leeds, United Kingdom; [38]Medical Genetics Service, Complejo Hospitalario de Navarra, Pamplona, Spain; [39]Genetic Department, Femme-Mère-Enfant Hospital, Hospices Civils de Lyon and INSERM U1028, CNRS UMR5292, Centre de Recherche en Neurosciences de Lyon, GENDEV Team, Université Claude Bernard Lyon 1, Bron, France; [40]Division of Pediatric Neurology, King Saud University, Riyadh, Kingdom of Saudi Arabia; [41]Medical Genetics Service, CHU Strasbourg, Strasbourg, France; [42]Department of Histology and Embryology, Faculty of Medicine, Near East University, Lefkoşa, Cyprus; [43]Department of Histology and Embryology, Faculty of Medicine, University of Uludag, Bursa, Turkey; [44]Department of Medical Genetics, Faculty of Medicine, University of Uludag, Bursa, Turkey; [45]Centre for Human Genetics, Université de Franche Comté, Besançon, France; [46]A Twist of Fate–ATS, Owasso, Oklahoma, USA; [47]Department of Anatomy and Cell Biology, McGill University, Montreal, Quebec, Canada. Correspondence: Bert Callewaert (bert.callewaert@ugent.be)
J.A. and A.B. share joint second authorship.

Submitted 11 June 2017; accepted 3 November 2017; advance online publication 11 January 2018. doi:10.1038/gim.2017.253

aortic segments). Paraffin-embedded samples were cut to 5-µm-thick samples, deparaffinized, and rinsed in distilled water. For Verhoeff–Van Gieson staining, sections were first immersed in Verhoeff's hematoxylin (5% alcoholic hematoxylin, 10% ferric chloride and Weigert's iodine) for 1 h and then washed. Next, sections were differentiated in 2%

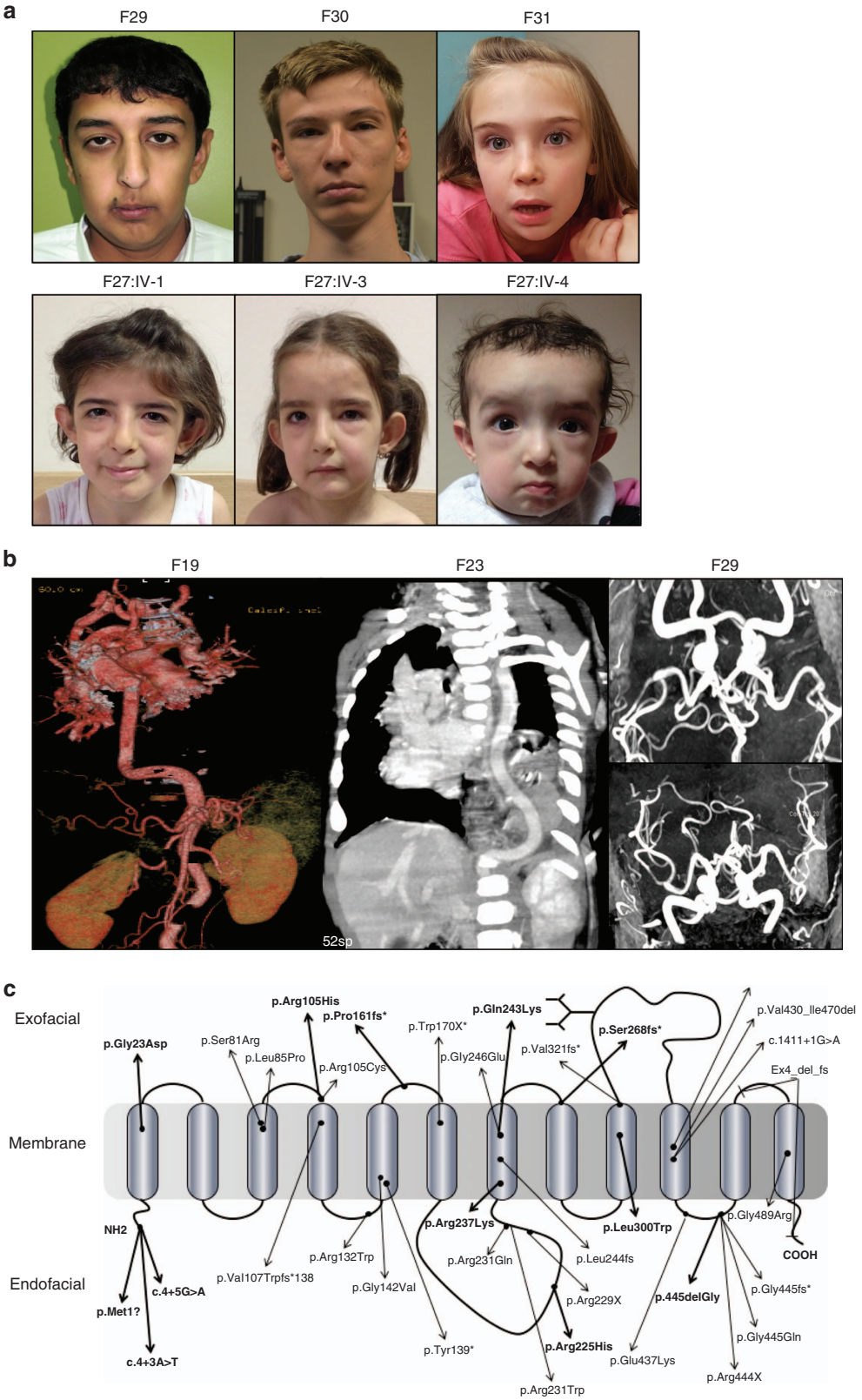

ferric chloride solution, microscopically checked for black fibers on a gray background, and rinsed in water. Iodine was removed using 5% sodium thiosulfate. After washing in water, sections were counterstained with Van Gieson's staining, dehydrated in ethanol, cleared in xylene, and mounted. For Picrosirius Red staining, samples were stained during 1 hour with Picrosirius Red F3B and a saturated aqueous solution of picric acid. After washing in two changes of acidified water, sections were dehydrated in ethanol, cleared in xylene, and mounted. For immunohistochemistry, epitope unmasking with citrate buffer (10 mM, pH 6) was followed by the inhibition of autoperoxidase activity with 3% H_20_2. Next, the sections were blocked with blocking serum (Vectastain Elite ABC-HRP Kit, Vector Laboratories Burlingame, CA, USA), followed by an overnight primary antibody incubation at 4 °C. Primary antibodies were directed against pSMAD2 (cat. nr. 3101, Cell Signaling Technology, Danvers, MA, USA) and CTGF (cat. nr. ab6992, Abcam, Cambridge, UK) and were used at a 1/200 dilution. Next, sections were incubated with a biotinylated secondary antibody, avidin–biotin complex (ABC) reagent and 3,3-diaminobenzidine peroxidase (Vectastain Elite ABC-HRP Kit, Vector Laboratories Burlingame, CA, USA). Subsequently, sections were counterstained with hematoxylin, dehydrated in ethanol, cleared in xylene, and mounted. All sections were visualized with a Zeiss Axio Observer Z1 microscope. For electron microscopy (EM), samples were fixed in a 4% formaldehyde (EM grade), 2.5% glutaraldehyde (EM grade), 0.1 M cacodylate buffer solution, stained en bloc with OsO_4 and uranyl acetate, and then dehydrated and embedded in Epon, as previously described.[22] Thin sections (60 nm) were cut, placed on formvar-coated grids, and counterstained with 7% methanolic uranyl acetate and lead citrate. Sections were viewed using a Tecnai 12 transmission electron microscope at 120 kV and images were digitally captured.

RESULTS

Demographic features

We report 40 newly identified ATS families. The male-to-female ratio of affected individuals is 27/22 ($p = 0.88$). The present age of the probands ranges from 1 to 30 years (mean 11.37 years, median 8 years). Age at diagnosis ranges from neonatal to 30 years (mean 4.84 years, median 2 years). Parental consanguinity was observed in 18 affected families. No mortality was observed in our cohort, although a sister of proband F11, retrospectively likely affected with ATS, died from complications of a diaphragmatic hernia.

Clinical presentation

The clinical characteristics of all patients are presented in **Supplementary Table S2**. First presentations initiating further investigation leading to the diagnosis are listed in **Table 1**. About half of all patients presented with cardiovascular manifestations, mostly coarctation of the isthmus aortae or a functional cardiac murmur for which echocardiography was requested. One patient showed aortic tortuosity on routine radiography for pneumonia. Six term probands manifested infant respiratory distress syndrome (IRDS), recovering well with standard neonatal care. Other presenting symptoms included skin abnormalities such as stretchable skin and cutis laxa, as well as gastrointestinal problems including failure to thrive and pyloric stenosis. Five patients were diagnosed upon familial segregation. Prenatal manifestations were evaluated in three probands and include the observation of aortic tortuosity, oligohydramnios, and intrauterine growth retardation.

Clinical manifestations

Most patients presented with typical craniofacial manifestations including a long face, hypertelorism, downslanting palpebral fissures, epicanthal folds, sagging cheeks, large ears, and a highly arched palate (**Figure 1a**). Four probands were diagnosed with a cleft palate or bifid uvula. About one-third of the patients appeared prematurely aged. Skeletal manifestations included joint laxity in most patients (36/42, 86%) with a mean Beighton score of 6.55/9 (range 5–9/9), pectus deformity (predominantly pectus excavatum) (17/45, 38%), arachnodactyly (15/47, 32%), and scoliosis (12/44, 27%). Several patients had muscular hypotonia. Ocular involvement included myopia (15/36, 42%) and five patients examined with automated keratometry and ultrasonic pachymetry showed corneal thinning (5/5), keratectasia (3/5), keratoconus (2/5), and keratoglobus (1/5).[23] Skin involvement ranged from a thin, hyperextensible skin with a velvety texture in the vast majority of patients to marked cutis laxa in 21 patients (51%). We did not observe any significant wound healing problems following surgery. Eleven patients had diaphragmatic hernias (34%), eight of which were surgically corrected. Eight patients presented with hiatal hernias (26%). Inguinal hernias were observed in one-third of the patients. Six patients had both inguinal and diaphragmatic hernias, and

Figure 1 Clinical and molecular characteristics. (**a**) Typical craniofacial features in six patients (F29, F30, F31, and the sisters F27:IV-1, F27:IV-3, F27:IV-4). Note a long face, hypertelorism, downslanting palpebral fissures, sagging cheeks, large ears, beaked nose. (**b**) Vascular imaging. Patient F19: 3D vascular imaging of the aorta and aortic side branches (frontal view) showing tortuosity of the aorta, supra-aortic, and pulmonary arteries. Patient F23: Thoracic and upper abdominal magnetic resonance imaging (frontal view) showing significant tortuosity of both the thoracic and abdominal aorta. Patient 29: Brain magnetic resonance imaging showing generalized tortuosity of the intracranial arteries. (Upper, transverse view; lower, anterior coronal view). (**c**) Cartoon of GLUT10 showing all currently identified mutations (newly identified mutations indicated in bold). GLUT10 contains 12 hydrophobic transmembrane domains (ovals) and a hydrophilic loop containing a potential *N*-linked glycosylation site between transmembrane domains 9 and 10.

Table 1 Initial presentations in our cohort

Initial presentation	Number of patients	Proband identification
Cardiovascular	**20**	
Aortic coarctation[a]	5	F4:III-4, F5, F14, F22, F25
Physiological cardiac murmur	8	F1, F4:III-1, F12:V-1, F15, F31, F32, F33, F35
Pulmonary hypertension	2	F21, F24
Pulmonary artery stenosis	1	F28
Aortic dilatation/ tortuosity	2	F13, F36
Cardiomyopathy	1	F29
Hypertension	1	F37:II-1
Respiratory	**7**	
Dyspnea and IRDS	6	F2, F3, F7, F9:II-1, F12:V-2, F20
Pulmonary infection	1	F19
Cutaneous	**7**	
Cutis laxa	4	F26:II-2, F27:IV-1, F27: IV-3, F27:IV-4
Stretchable skin	3	F18, F40:II-1, F40:II-2
Gastrointestinal	**2**	
Pyloric stenosis	1	F23
Failure to thrive	1	F11
Other	**1**	
Gross motor delay	1	F16
Segregation analysis	**5**	F9:II-2, F26:II-3, F26:II-4, F26:II-5, F37:II-2
Unknown presentation	**8**	F6, F8, F10, F17, F30, F34, F38, F39
Overall total	**50**	

IRDS, infant respiratory distress syndrome.
[a]Aortic coarctation presenting as circulatory failure (F4:III-4), absent femoral pulses (F5), variable blood pressure between the right arm and leg (F14), or systemic hypertension (F22).

five patients had umbilical hernias. Feeding difficulties were noted in five patients and four patients had a pyloric stenosis. Eight patients were diagnosed with renal and urinary tract abnormalities, of which three showed dilation of the pyelocaliceal system.

Cardiovascular manifestations

Tortuosity of the aorta and/or midsized arteries was invariably present (**Figure 1b**, **Supplementary Table S1**) and six patients had an abnormal implantation of the aortic side-branches. Tortuosity mostly affected the head, neck, and pulmonary arteries (48%). One patient had tortuous retinal arteries (F15). Five infants presented with aggressive aortic root aneurysm formation between the ages of 12 months and 3 years 8 months, with a diameter at diagnosis ranging from 21.8 to 60 mm (mean of 31.7 mm) requiring immediate repair. Four other patients were diagnosed with an aortic root aneurysm later on. *Z*-scores ranged from 2.95 to 7.22. One patient (F22) underwent surgical repair for an abdominal aortic aneurysm at the age of 15 months. Arterial dissections did not occur in this series. Aortic coarctation at the isthmus (**Table 1**) or the abdominal aorta occurred in respectively five and three patients. Two patients had a stenosis of a renal artery. Other vascular stenoses were present in more than half of patients, mostly affecting the pulmonary arteries (51% of patients). Mild to moderate systolic hypertension was present in 4/18 patients. In the neonatal period, patient F3 was diagnosed with a grade II intraventricular and parenchymal hemorrhage with diffuse ischemic changes in the brain. Patient F2 suffered from a stroke of unknown etiology resulting in left hemiparesis. Two patients had an intestinal perforation, which was likely caused by critical mesenteric artery stenosis.

Venous anomalies including tortuosity, early varicosities, femoral vein occlusion and dilatations of large veins (pulmonary, mesenteric, splenic, portal, and subhepatic veins) were sporadically present.

Right and/or left ventricular hypertrophy and dilatation was associated with pulmonary artery stenosis or aortic stenoses, respectively. Mitral valve prolapse was present in patient F8.

Molecular analysis

A total of 23 different mutations were found, of which 12 are previously unreported (**Figure 1c**). Of the 23 *SLC2A10* mutations identified in this series, there were 13 missense mutations, 3 nonsense mutations, 2 splice-site mutations, and 5 small deletions leading to a frameshift. For the novel mutations, the pathogenicity classification and CADD[24] score are represented in the **Supplementary Table S2**. We did not observe any genotype–phenotype correlations.

Histology

Verhoeff–Van Gieson staining on pulmonary and aortic biopsies in respectively patients F12:V-2, F21, F34, and patient F22 reveals disorganization of the elastic fibers. We observe a reduction of smooth elastic lamella, with highly disorganized, thicker, and more fragmented elastic fibers in vascular tissue. Elastic fiber fragmentation is more pronounced in aortic tissue. Picrosirius Red polarization staining shows increased and disorganized collagen deposition compared with the control samples (**Figure 2**). These findings were recapitulated on skin biopsies of ATS patients F33 and F34 showing few and disorganized elastic fibers compared with an age- and sex-matched control sample (**Supplementary Figure S1**).

Transmission electron microscopy of an elastic fiber in a control skin biopsy demonstrates a solid, dense core of elastin surrounded by a sparse mantle of microfibrils. In contrast, elastic fibers observed in the skin of ATS patients show abnormal ultrastructure, when compared with control elastic fibers. In ATS patient F30, although some elastin is solid and forms a core, the elastin in the periphery of the fiber is fragmented and infiltrated with microfibrils. In ATS patients F33 and F34, the elastin fiber core is disrupted by the presence of microfibrils, and an extensive, peripheral mantle of

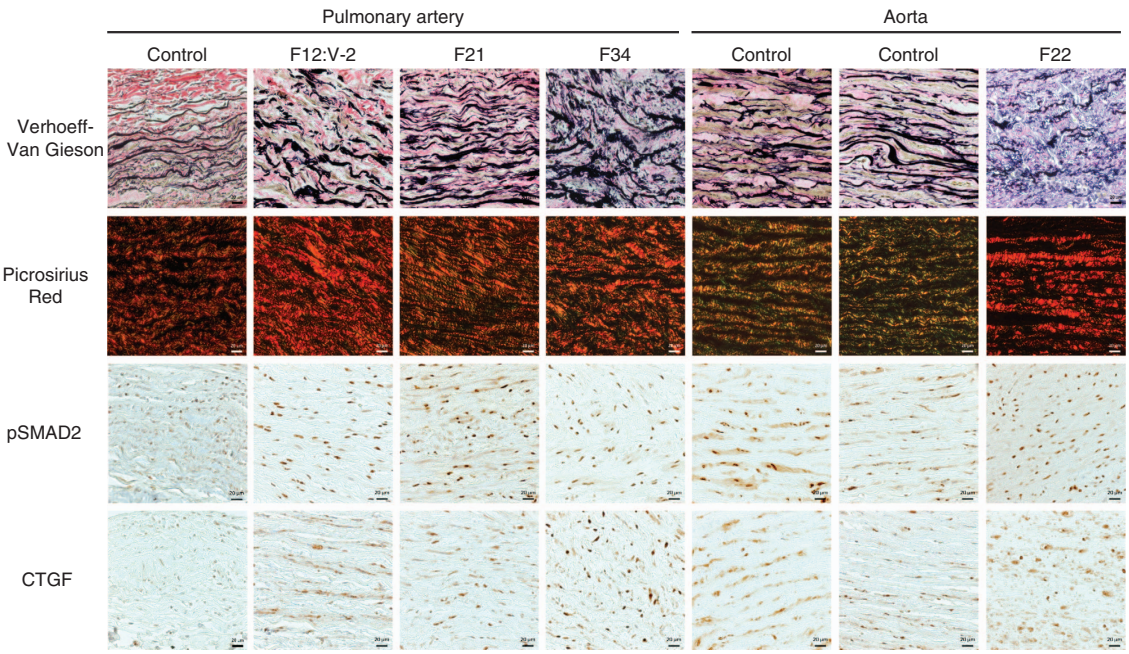

Figure 2 Histology and immunostaining of vascular biopsies of arterial tortuosity syndrome patients. (Immuno)stainings of pulmonary artery biopsies (patients F12:V-2, F21, and F34), and an aortic biopsy (patient F22) with Verhoeff–Van Gieson staining (row 1), Picrosirius Red polarization staining (row 2), immunostaining for pSMAD2 (row 3), and CTGF (row 4). The pictures are representative images of the central region of the medial layer of the artery. Bars = 20 μm.

microfibrils, of random directionality, can also be seen (**Figure 3**).

TGF-β signaling

Neither skin nor end-stage diseased arterial samples show evidence of altered pSMAD2 and CTGF staining compared with controls (**Figure 2**, **Supplementary Figure S1**).

DISCUSSION

This study describes the largest patient cohort with a molecularly confirmed diagnosis of ATS reported to date. Mutations in *SLC2A10* are spread throughout the gene, but missense mutations locate almost exclusively in the transmembrane and endofacial domains. This suggests that the critical passage of the substrate through the transporter locates at the endofacial side. Furthermore, the absence of mutations in the large exofacial loop between transmembrane domain 9 and 10 suggests a less critical role for this GLUT10-specific domain.

Initial case reports and generalized arterial anomalies in ATS suggested a poor prognosis.[7] Causes of death, though frequently unknown, were reported to include pulmonary infection,[7] myocarditis,[2] and organ infarctions.[5,7,8] Similar to a previous report,[15] the prognosis in this cohort seems more favorable, but differs significantly among individuals. However, the lack of natural history data precludes evidence-based management of patients.

The clinical data in this study are largely in line with previously reported series (**Table 2**). In our series, 21% developed aortic root dilatation at the level of the sinuses of Valsalva, which is more common than what has been reported in the literature (10%). The occurrence of early aneurysm formation of the aortic root at a young age in this series warrants initial echocardiographic follow-up at least every 3 months until the age of 5 years. After that, echocardiographic follow-up can be tailored to the findings but should continue at least annually as progressive dilatation may occur later in life.[7,15] Despite the progressive nature and sometimes large sizes of the aneurysms, no arterial dissections have been unequivocally recorded in ATS.[15] This, together with the amenability to vascular surgery, suggests that an aggressive surgical approach might not be indicated in cases of slowly progressive aortic root dilatation and that management guidelines similar to those being used for Marfan syndrome might be appropriate. About two-thirds of all patients have pulmonary artery stenoses, leading to feeding difficulties and pulmonary hypertension, requiring recurrent catheterizations with ballooning or stenting, and/or surgical interventions. Ischemic cerebrovascular events, as previously reported,[15] remain a concern, as this report adds a third case. Of note, two patients had an intestinal perforation likely secondary to local ischemia, similar to another reported case.[5] Coarctation at the isthmus is amenable to standard coarctectomy and end-to-end anastomosis or stenting in milder cases. Larger stenotic stretches of the aorta may occur and may result in left ventricular hypertrophy. Importantly, this cohort confirms that a minority of patients (26%) may show stenoses distal to the aortic isthmus or in the aortic side branches,

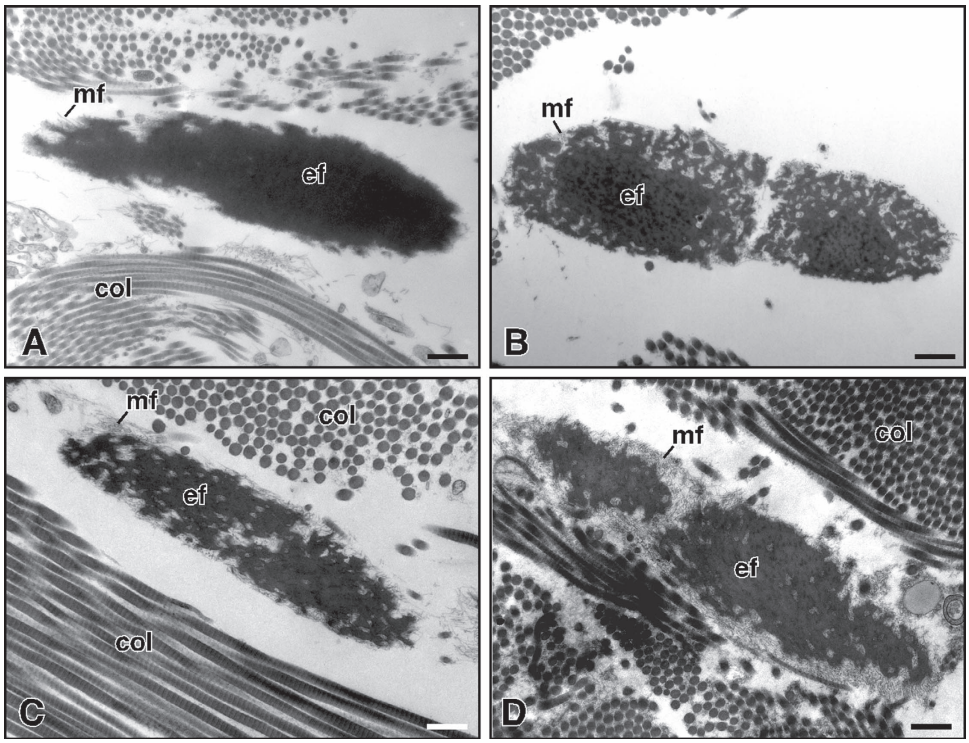

Figure 3 Electron microscopic findings in arterial tortuosity syndrome. (**a**) Transmission electron microscopy of elastic fibers in a control skin biopsy. (**b**–**d**) Representative image of an elastic fiber of arterial tortuosity syndrome patients (**b**) F30, (**c**) F34, and (**d**) F33. Bars = 500 nm. col, collagen fiber; ef, elastic core; mf, microfibrils.

including the abdominal aorta, superior mesenteric artery and the renal arteries. Therefore, caution is warranted when starting agents that interfere with intraglomerular pressure such as angiotensin-converting enzyme inhibitors, angiotensin II receptor 1 antagonists, and nonsteroidal anti-inflammatory agents.

Prenatal manifestations include intrauterine growth retardation, oligohydramnios, and aortic tortuosity. We noticed a high incidence of IRDS and diaphragmatic hernias. IRDS can result from a diaphragmatic hernia, but may also relate directly to GLUT10 deficiency. Indeed, GLUT10 is highly expressed in lung alveoli and has been associated with airway sterility.[25] It also has been recognized that other elastinopathies, including Marfan and Loeys–Dietz syndromes, may show perturbed development of alveoli. Other presentations in infancy were pyloric stenosis and failure to thrive. Failure to thrive is often associated with pulmonary artery stenosis. Pyloric stenoses have also been reported in other elastinopathies that may cause vascular stenoses including LTBP4 deficiency.[26] All patients presented with characteristic facial features and variable connective tissue disorder manifestations including increased skin laxity, hernias (diaphragmatic, inguinal, and umbilical), joint hypermobility, and muscular hypoplasia. These connective tissue disorder manifestations are important as diagnostic triggers, but also because they may affect quality of life due to joint pain and exercise intolerance. We confirmed that when being examined carefully by automated keratometry and ultrasonic pachymetry, many patients show corneal thinning that may evolve to keratoconus,[15,27] keratoglobus, or corneal ectasia.[23]

We demonstrate elastic fiber fragmentation and increased collagen deposition in both skin and vascular biopsies of ATS patients. In contrast to a previous report,[16] immunohistochemical staining for CTGF and nuclear pSMAD2 in arterial tissue and skin biopsies did not unequivocally evidence upregulation of the TGF-β signaling pathway. TGF-β signaling is upregulated in many elastic fiber diseases including Loeys–Dietz, Marfan, and several cutis laxa syndromes,[28–31] but the exact spatiotemporal regulation of TGF-β signaling remains a matter of debate. Indeed, in a morpholino zebrafish model of ATS, TGF-β signaling is downregulated during the first days of development.[20] In addition, TGF-β signaling alterations can either be a *primum movens* of altered matrix homeostasis or occur secondary to altered TGF-β sequestration in the matrix or altered matrix stiffness. Moreover, upregulation of TGF-β signaling may be protective in the early phase of aneurysm formation, as evidenced by outcome differences when treating aneurysm progression in Marfan mice models with TGF-β inhibition before or after the onset of aneurysm formation.[32] Also, treatment of children and young adults with Marfan syndrome and prominent aortic root dilatation with losartan, a TGF-β antagonist, was not beneficial compared with treatment with atenolol.[33] Our observations, based on a

Table 2 Overview of the phenotypic presentation in this cohort and the patients reported in literature

	This series	Literature	Total	
	Patients ($n = 50$)	Patients ($n = 52$)	Probands ($n = 78$)	Patients ($n = 102$)
M/F ratio	27/22 (54%/44%)	29/22 (56%/42%)	45/30 (58%/38%)	56/44 (55%/43%)
Parental consanguinity	24/48 (50%)	31/51 (61%)	35/75 (47%)	55/99 (56%)
Craniofacial				
Aged appearance	13/35 (37%)	6/25 (24%)	11/41 (27%)	19/60 (32%)
Long face	32/49 (65%)	35/43 (81%)	51/64 (80%)	67/92 (73%)
Hypertelorism	14/35 (40%)	9/47 (19%)	13/68 (19%)	23/82 (28%)
Downslanting palpebral fissures	25/44 (64%)	13/47 (28%)	21/65 (32%)	38/91 (42%)
Beaked nose	22/45 (49%)	11/45 (24%)	27/62 (44%)	33/90 (37%)
Cleft palate/bifid uvula	4/47 (9%)	3/49 (6%)	3/66 (5%)	7/96 (7%)
High arched palate	29/44 (66%)	14/43 (32%)	31/59 (53%)	43/87 (49%)
Micrognathia	23/45 (51%)	29/45 (64%)	35/65 (54%)	52/90 (58%)
Sagging cheeks	27/49 (55%)	24/46 (52%)	37/62 (60%)	51/95 (54%)
Ocular				
Keratoconus	3/38 (8%)	5/17 (29%)	6/38 (15%)	8/55 (15%)
Keratoglobus	0/38 (0%)	2/17 (12%)	2/38 (5%)	2/55 (4%)
Myopia	15/36 (42%)	8/17 (47%)	17/39 (44%)	23/53 (43%)
Cutaneous				
Velvety texture	26/41 (63%)	12/45 (27%)	28/51 (55%)	38/86 (44%)
Thin skin	17/43 (40%)	5/42 (12%)	15/50 (30%)	22/85 (26%)
Hyperextensible skin	27/46 (50%)	29/46 (63%)	41/55 (75%)	56/92 (61%)
Cutis laxa	21/41 (51%)	6/46 (13%)	20/63 (32%)	27/87 (31%)
Skeletal				
Pectus deformity	17/45 (38%)	9/47 (19%)	20/67 (30%)	26/92 (28%)
Scoliosis	12/44 (27%)	8/46 (17%)	12/65 (18%)	20/90 (22%)
Arachnodactyly	15/47 (32%)	13/45 (29%)	16/66 (24%)	28/93 (30%)
Joint laxity	36/42 (86%)	36/53 (68)	51/72 (71%)	72/95 (76%)
Joint pain	8/32 (21%)	2/37 (5%)	6/48 (13%)	10/69 (26%)
Cardiovascular				
Aortic tortuosity	37/41 (90%)	46/49 (94%)	65/70 (93%)	83/90 (92%)
Tortuosity of other arteries	38/42 (90%)	35/49 (71%)	68/72 (94%)	73/91 (80%)
Abnormal implantation of the aortic branches	6/42 (14%)	5/46 (11%)	10/67 (15%)	11/88 (13%)
Aortic root aneurysm	9/42 (21%)	5/48 (10%)	9/66 (14%)	14/90 (16%)
Other arterial aneurysms	8/37 (22%)	3/50 (6%)	7/65 (11%)	11/87 (13%)
Arterial dissections	0/37 (0%)	0/50 (0%)	0/64 (0%)	0/87 (0%)
Stenosis of the pulmonary arteries	23/42 (55%)	29/49 (59%)	42/68 (62%)	52/91 (57%)
Aortic stenosis	11/41 (27%)	11/49 (22%)	17/67 (25%)	22/90 (24%)
Other stenoses	10/38 (26%)	2/43 (5%)	9/60 (15%)	12/81 (15%)
Other manifestations				
Diaphragmatic hernia	11/32 (34%)	8/33 (24%)	15/42 (36%)	19/65 (29%)
Inguinal hernia	19/45 (42%)	16/47 (34%)	27/65 (42%)	35/92 (38%)
Respiratory symptoms	7/45 (16%)	3/22 (14%)	15/74 (20%)	10/67 (15%)
Urogenital abnormalities	8/37 (22%)	3/19 (16%)	8/41 (20%)	11/56 (20%)
Autonomic dysfunction	5/31 (16%)	6/26 (23%)	5/37 (14%)	10/57 (18%)

F, female; M, male.

limited number of samples, indicate that the exact contribution of TGF-β signaling in the etiology of vascular tortuosity and aneurysm formation needs further exploration.

We are the first to report on transmission electron microscopy in ATS. Dermal elastic fibers show a distinct and recognizable pattern with poorly organized elastin assembly, especially at the periphery of the elastic fiber, where a large mantle of bare microfibrils is observed. Though we could not verify this in vascular tissue, it is tempting to speculate that reduced deposition of mature elastin in the extracellular matrix may lead to increased vascular smooth muscle cell proliferation and stenosis formation. As a whole,

our clinical, histological, and ultrastructural observations suggest that GLUT10 deficiency affects the extracellular matrix homeostasis, rather than elastin alone.

In conclusion, this series confirms a better prognosis than initially reported in ATS, but warrants close follow-up for early aortic aneurysm formation and stenoses during the first years. These results shed light on previously unknown features such as prenatal manifestations, IRDS, and corneal thinning. In addition, early and aggressive aneurysm formation, diaphragmatic hernia, and ischemic events remain a concern. To provide a full diagnostic work-up and early recognition of complications, we would suggest to perform a detailed clinical examination, echocardiography, "head-to-pelvis" nuclear magnetic resonance angiography, ophthalmological examination with keratometry, and renal artery ultrasound in every patient diagnosed with ATS.

SUPPLEMENTARY MATERIAL

Supplementary material is linked to the online version of the paper at http://www.nature.com/gim

ACKNOWLEDGMENTS

M.A.S. was supported by the Deanship of Scientific Research, King Saud University, Riyadh, Saudi Arabia (research group RGP-VPP-301). A.B. is supported by the Special Research Fund, Flanders of Ghent University (grant 01N04516 to B.C.). E.C.D is supported by a Natural Sciences and Engineering Research Council of Canada grant (NSERC RGPIN 355710) and acknowledges the technical assistance of the Facility for Electron Microscopy Research at McGill University. B.C. is a senior clinical investigator of the Research Foundation–Flanders. This study is supported by the Special Research Fund of Ghent University to A. D.P. (grant BOF14/01M01108) and the Research Foundation–Flanders (grant FWOOPR2013025301 to P.C., A.W., and B.C.). We are thankful to all families and patients for their interest and participation.

DISCLOSURE

The authors declare no conflict of interest.

REFERENCES

1. Abdul Wahab A, Janahi IA, Eltohami A, Zeid A, Faiyaz Ul Haque M, Teebi AS. A new type of Ehlers-Danlos syndrome associated with tortuous systemic arteries in a large kindred from Qatar. *Acta Paediatr* 2003;92:456–62.
2. Ades LC, Knight WB, Byard RW, et al. Clinicopathologic findings in congenital aneurysms of the great vessels. *Am J Med Genet*. 1996;66:289–99.
3. Al Fadley F, Al Manea W, Nykanen DG, Al Fadley A, Bulbul Z, Al Halees Z. Severe tortuosity and stenosis of the systemic, pulmonary and coronary vessels in 12 patients with similar phenotypic features: a new syndrome? *Cardiol Young* 2000;10:582–9.
4. Lees MH, Menashe VD, Sunderland CO, Mgan CL, Dawson PJ. Ehlers-Danlos syndrome associated with multiple pulmonary artery stenoses and tortuous systemic arteries. *J Pediatr* 1969;75:1031–6.
5. Pletcher BA, Fox JE, Boxer RA, et al. Four sibs with arterial tortuosity: description and review of the literature. *Am J Med Genet*. 1996;66:121–8.
6. Welch JP, Aterman K, Day E, Roy DL. Familial aggregation of a "new" connective-tissue disorder: a nosologic problem. *Birth Defects Orig Artic Ser*. 1971;7:204–13.
7. Wessels MW, Catsman-Berrevoets CE, Mancini GM, et al. Three new families with arterial tortuosity syndrome. *Am J Med Genet A*. 2004;131:134–43.
8. Beuren AJ, Hort W, Kalbfleisch H, Muller H, Stoermer J. Dysplasia of the systemic and pulmonary arterial system with tortuosity and lengthening of the arteries. A new entity, diagnosed during life, and leading to coronary death in early childhood. *Circulation* 1969;39:109–15.
9. Ertugrul A. Diffuse tortuosity and lengthening of the arteries. *Circulation* 1967;36:400–7.
10. Gardella R, Zoppi N, Assanelli D, Muiesan ML, Barlati S, Colombi M. Exclusion of candidate genes in a family with arterial tortuosity syndrome. *Am J Med Genet A*. 2004;126A:221–8.
11. Meyer S, Faiyaz-Ul-Haque M, Zankl M, et al. [Arterial tortuosity syndrome]. *Klin Padiatr.* 2005;217:36–40.
12. Rivera IR, Gomes L, Moises VA, Silva CC, Andrade JL, Carvalho AC. Multiple arterial anomalies in the newborn infant. Echocardiographic and angiographic diagnosis. *Arq Bras Cardiol*. 2000;75:137–44.
13. Zaidi SH, Peltekova V, Meyer S, et al. A family exhibiting arterial tortuosity syndrome displays homozygosity for markers in the arterial tortuosity locus at chromosome 20q13. *Clin Genet*. 2005;67:183–8.
14. Franceschini P, Guala A, Licata D, Di Cara G, Franceschini D. Arterial tortuosity syndrome. *Am J Med Genet*. 2000;91:141–3.
15. Callewaert BL, Willaert A, Kerstjens-Frederikse WS, et al. Arterial tortuosity syndrome: clinical and molecular findings in 12 newly identified families. *Hum Mutat* 2008;29:150–8.
16. Coucke PJ, Willaert A, Wessels MW, et al. Mutations in the facilitative glucose transporter GLUT10 alter angiogenesis and cause arterial tortuosity syndrome. *Nat Genet* 2006;38:452–7.
17. Lee YC, Huang HY, Chang CJ, Cheng CH, Chen YT. Mitochondrial GLUT10 facilitates dehydroascorbic acid import and protects cells against oxidative stress: mechanistic insight into arterial tortuosity syndrome. *Hum Mol Genet*. 2010;19:3721–33.
18. Loeys BL, Chen J, Neptune ER, et al. A syndrome of altered cardiovascular, craniofacial, neurocognitive and skeletal development caused by mutations in TGFBR1 or TGFBR2. *Nat Genet* 2005;37:275–81.
19. Loeys BL, Schwarze U, Holm T, et al. Aneurysm syndromes caused by mutations in the TGF-beta receptor. *N Engl J Med*. 2006;355:788–98.
20. Willaert A, Khatri S, Callewaert BL, et al. GLUT10 is required for the development of the cardiovascular system and the notochord and connects mitochondrial function to TGFβ signaling. *Human Molecular Genetics*. 2012;21(16):1248–59. doi:10.1093/hmg/ddr555.
21. Moceri P, Albuisson J, Saint-Faust M, et al. Arterial tortuosity syndrome: early diagnosis and association with venous tortuosity. *J Am Coll Cardiol*. 2013;61:783.
22. Davis EC. Smooth muscle cell to elastic lamina connections in developing mouse aorta. Role in aortic medial organization. *Lab Invest* 1993;68(1):89–99.
23. Hardin JS, Zarate YA, Callewaert B, Phillips PH, Warner DB. Ophthalmic findings in patients with arterial tortuosity syndrome and carriers: a case series. *Ophthalmic Genet* 2018;39:29–34.
24. Kircher M, Witten DM, Jain P, O'Roak BJ, Cooper GM, Shendure J. A general framework for estimating the relative pathogenicity of human genetic variants. *Nat Genet* 2014;46:310–315.
25. Pezzulo AA, Gutierrez J, Duschner KS, et al. Glucose depletion in the airway surface liquid is essential for sterility of the airways. *PLoS One* 2011;6:e16166.
26. Callewaert B, Su CT, Van Damme T, et al. Comprehensive clinical and molecular analysis of 12 families with type 1 recessive cutis laxa. *Hum Mutat* 2013;34:111–21.
27. Hasler S, Sturmer J, Kaufmann C. Keratoglobus and deep stromal corneal opacification in a case of arterial tortuosity syndrome. *Klin Monbl Augenheilkd*. 2011;228:345–6.
28. Loeys BL, Schwarze U, Holm T, et al. Aneurysm syndromes caused by mutations in the TGF-beta receptor. *N Engl J Med*. 2006;355:788–98.
29. Neptune ER, Frischmeyer PA, Arking DE, et al. Dysregulation of TGF-beta activation contributes to pathogenesis in Marfan syndrome. *Nat Genet* 2003;33:407–11.
30. Callewaert B, Renard M, Hucthagowder V, et al. New insights into the pathogenesis of autosomal-dominant cutis laxa with report of five ELN mutations. *Hum Mutat* 2011;32:445–55.

31. Renard M, Holm T, Veith R, et al. Altered TGFbeta signaling and cardiovascular manifestations in patients with autosomal recessive cutis laxa type I caused by fibulin-4 deficiency. *Eur J Hum Genet*. 2010;18:895–901.
32. Cook JR, Clayton NP, Carta L, et al. Dimorphic effects of transforming growth factor-beta signaling during aortic aneurysm progression in mice suggest a combinatorial therapy for Marfan syndrome. *Arterioscler Thromb Vasc Biol*. 2015;35:911–7.
33. Lacro RV, Dietz HC, Sleeper LA, et al. Atenolol versus losartan in children and young adults with Marfan's syndrome. *N Engl J Med*. 2014;371: 2061–71.